ORIGINAL ARTICLE

Basic Study

Near-infrared photoimmunotherapy of pancreatic cancer using an indocyanine green-labeled anti-tissue factor antibody

Winn Aung, Atsushi B Tsuji, Aya Sugyo, Hiroki Takashima, Masahiro Yasunaga, Yasuhiro Matsumura, Tatsuya Higashi

Winn Aung, Atsushi B Tsuji, Aya Sugyo, Tatsuya Higashi, Department of Molecular Imaging and Theranostics, National Institute of Radiological Sciences, National Institutes for Quantum and Radiological Science and Technology (QST-NIRS), Chiba 263-8555, Japan

Hiroki Takashima, Masahiro Yasunaga, Yasuhiro Matsumura, Division of Developmental Therapeutics, Exploratory Oncology Research and Clinical Trial Center, National Cancer Center, Chiba 277-8577, Japan

ORCID number: Winn Aung (0000-0002-0896-7158); Atsushi B Tsuji (0000-0003-2726-288X); Aya Sugyo (0000-0002-5174-4478); Hiroki Takashima (0000-0001- 6487-7344); Masahiro Yasunaga (0000-0002-5712-9847); Yasuhiro Matsumura (0000-0003-4331-8177); Tatsuya Higashi (0000-0002-8338-4737).

Abstract

AIM

To investigate near-infrared photoimmunotherapeutic effect mediated by an anti-tissue factor (TF) antibody conjugated to indocyanine green (ICG) in a pancreatic cancer model.

METHODS

Near-infrared photoimmunotherapy (NIR-PIT) is a highly selective tumor treatment that utilizes an antibody-photosensitizer conjugate administration, followed by NIR light exposure. Anti-TF antibody 1849-ICG conjugate was synthesized by labeling of rat IgG_{2b} anti-TF monoclonal antibody 1849 (anti-TF 1849) to a NIR photosensitizer, ICG. The expression levels of TF in two human pancreatic cancer cell lines were examined by western blotting. Specific binding of the 1849-ICG to TF-expressing BxPC-3 cells was examined by fluorescence microscopy. NIR-PIT-induced cell death was determined by cell viability imaging assay. *In vivo* longitudinal fluorescence imaging was used to explore the accumulation of 1849-ICG conjugate in xenograft tumors. To examine the effect of NIR-PIT, tumor-bearing mice were separated into 5 groups: (1) 100 μg of 1849-ICG i.v. administration followed by NIR light exposure (50 J/cm^2) on two consecutive days (Days 1 and 2); (2) NIR light exposure (50 J/cm^2) only on two consecutive days (Days 1 and 2); (3) 100 μg of 1849-ICG i.v. administration; (4) 100 μg of unlabeled anti-TF 1849 i.v. administration; and (5) the untreated control. Semiweekly tumor volume measurements, accompanied with histological and immunohistochemical (IHC) analyses of tumors, were performed 3 d after the 2nd irradiation with NIR light to monitor the effect of treatments.

RESULTS

High TF expression in BxPC-3 cells was observed *via* western blot analysis, concordant with the observed preferential binding with intracellular localization of 1849-ICG *via* fluorescence microscopy. NIR-PIT-induced cell death was observed by performing cell viability imaging assay. In contrast to the other test groups, tumor growth was significantly inhibited by NIR-PIT with a statistically significant difference in relative tumor volumes for 27 d after the treatment start date [2.83 ± 0.38 (NIR-PIT) *vs* 5.42 ± 1.61 (Untreated), *vs* 4.90 ± 0.87 (NIR), *vs* 4.28 ± 1.87 (1849-ICG), *vs* 4.35 ± 1.42 (anti-TF 1849), at Day 27, $P < 0.05$]. Tumors that received NIR-PIT showed evidence of necrotic cell death-associated features upon hematoxylin-eosin staining accompanied by a decrease in Ki-67-positive cells (a cell proliferation marker) by IHC examination.

CONCLUSION

The TF-targeted NIR-PIT with the 1849-ICG conjugate can potentially open a new platform for treatment of TF-expressing pancreatic cancer.

Core tip: We examined whether anti-tissue factor (TF) antibody 1849-indocyanine green (ICG) conjugate (1849-ICG) induced the photoimmunotherapeutic effect in a pancreatic cancer xenograft. There was no report about employing 1849-ICG conjugate which selectively binds the target antigen TF for near-infrared photoimmunotherapy (NIR-PIT) of tumor, though some studies have suggested the usefulness of anti-TF 1849 in cancer imaging and therapy. Our study proposes for the first time that 1849-ICG conjugate is a desirable candidate for new treatment modality NIR-PIT of pancreatic cancer after evaluating its cytotoxic and antitumor effects *via in vitro* and *in vivo* studies in mouse model of pancreatic cancer.

INTRODUCTION

Pancreatic cancer is one of the most devastating health issues that has caused 411600 deaths, globally, in 2015 for all ages and both sexes[1]. In 2018, in the United States, it is the fourth and ninth leading cancer type for estimated cancer death and new cancer case, respectively[2]. Pancreatic cancer has the lowest 5-year survival rate of 8%, for all stages combined[2]. The major reasons of poor prognosis are late diagnosis and lack of effective therapy. Therefore, for achieving early diagnosis and new treatment options, the efficacious antibody based molecular-targeting therapeutic approaches are currently gaining attention in preclinical and clinical research. Conventional immunotherapy itself as well as using certain antibodies, antibody-drug conjugate (ADC) therapy, radioimmunotherapy (RIT), and photoimmunotherapy (PIT) are being investigated substantially. Meanwhile, the effort to explore a novel target molecule and a suitable theranostic agent is still imperative.

Tissue factor (TF) is a 47-kDa single chain transmembrane glycoprotein belonging to the cytokine receptor family group 2, composed of 263 amino acid residues. TF mediates a variety of physiologically- and pathophysiologically-relevant functions and its overexpression is linked to thrombogenicity, tumor angiogenesis, cell signaling, tumor cell proliferation, and metastasis[3-5]. Various malignant entities including pancreatic cancer has shown the expression of TF[6,7]. Moreover, in contrast

to normal pancreas with low TF expression, a high TF expression in pancreatic cancer correlates with tumor grade, extent, metastasis and invasion[6,8,9]. Haas and co-workers have previously analyzed the expression of TF in eight human pancreatic cancer cell lines including BxPC-3 and reported presence of TF expression, at RNA and protein level. Corresponding to the TF expression in cell lines, they also demonstrated that most of the tissue specimens of pancreatic cancer patients have highly variable TF expression, as determined by immuno-fluorescence staining[10]. Previously, we suggested that TF may be a promising target for cancer diagnostic imaging or therapy, developed several anti-TF antibodies, and showed that a rat IgG2b anti-TF monoclonal antibody 1849 has high affinity against TF[11,12]. We reported the development of Alexa Flour-647-labeled anti-TF antibody 1849 probe for fluorescence imaging in a TF-overexpressing human pancreatic cancer xenograft model[11] and an ^{111}In-labeled anti-TF antibody 1849 probe for immuno- single-photon emission computed tomography (SPECT) imaging in glioma model[13] and pancreatic cancer models (manuscript under preparation). Cai *et al*[14,15] have successfully developed a radiotracer for immuno-PET (positron emission computed tomography) imaging of *in vivo* TF expression in pancreatic cancer and breast cancer models[16]. Wang *et al*[17] labeled anti-TF antibody with ^{90}Y and reported its radiotherapeutic effect on human xenograft NSCLC tumors in nude mice. These studies that considered TF as a molecular target encourage us to use anti-TF antibody 1849 in near-infrared PIT (NIR-PIT).

NIR-PIT is a modified version of the conventional photodynamic therapy (PDT) or photothermal therapy (PTT). NIR-PIT exerts a target cell specific cancer treatment that enables highly selective cell death after systemic administration of a photosensitizer-conjugated antibody against tumor-associated antigens, and accompanying exposure with NIR light. The light of a specific wavelength activates the relevant photosensitizer, and this interaction induces a cytotoxic reaction. An antibody which binds a cancer specific antigen expressing on the cellular membrane, is desirable for selective targeting of cancer cells. Over recent decades, a wide variety of available monoclonal antibodies that bind to the various molecular targets, have been considered and used with NIR-PIT in preclinical studies by several research groups. Among them, NIR-PIT using anti-epidermal growth factor receptor (EGFR) antibody (cetuximab) conjugated to a photosensitizer, phthalocyanine dye IRDye® 700DX NHS Ester (IR700DX), has been widely studied and is currently in its Phase I/II clinical study (study of RM-1929 and PIT in patients with recurrent head and neck cancer: NCT02422979).

In the present study, we conjugate an anti-TF monoclonal antibody 1849 with a photosensitizer, indocyanine green (ICG), and demonstrate the potential of the generated 1849-ICG conjugate as a desirable candidate for NIR-PIT of pancreatic cancer, after evaluating its cytotoxic and antitumor effects *via in vitro* and *in vivo* studies in a mouse model of pancreatic cancer.

MATERIALS AND METHODS

Cell lines
The human pancreatic cancer cell lines, BxPC-3 and SUIT-2, were purchased from the ATCC (Manassas, VA, United States). BxPC-3 cells were maintained in RPMI 1640 medium (Sigma-Aldrich, St. Louis, MO, United States) supplemented with 10% fetal bovine serum (FBS) (Nichirei Biosciences, Tokyo, Japan), 100 U/mL penicillin-G sodium, and 100 mg/mL streptomycin sulfate (Invitrogen, Carlsbad, CA, United States) at 37 ℃ under a humidified atmosphere containing 5% CO_2. SUIT-2 cells were maintained in high glucose Dulbecco's modified Eagle's medium (DMEM) (Wako, Osaka, Japan) supplemented with 10% FBS, 100 U/mL penicillin, and 100 μg/mL streptomycin.

Western blot analysis
Western blotting was performed to analyze TF expression in cultured cells. Whole-cell lysates were prepared using radioimmunoprecipitation assay buffer (Wako Pure Chemical Industries, Osaka, Japan) supplemented with a protease inhibitor cocktail (Sigma-Aldrich). Total protein concentration was measured using a NanoDrop One spectrophotometer (Thermo Fisher Scientific, Wilmington, DE, United States). Protein samples (35 μg) were separated on a 4%-20% polyacrylamide gel (ATTO Corporation, Tokyo, Japan) and transferred on to Immobilon-P membrane (Millipore, Billerica, MA, United States). As primary antibodies, anti-TF 1849 (generated by us) and a commercially available goat anti-human actin (C-11) antibody (Santa Cruz Biotechnology, Santa Cruz, CA, United States), were used. A horseradish peroxidase (HRP)-linked anti-rabbit IgG antibody and anti-rat IgG antibody (GE Healthcare, Little Chalfont, United Kingdom) were used as the secondary antibodies. Immunoreactive bands were visualized using the Enhanced Chemiluminescence Plus Western blotting detection system (GE Healthcare).

Photosensitizer labeling of anti TF-antibody
The rat IgG2b anti-TF monoclonal antibody 1849 which reacts with human TF antigen was developed as previously described[12]. An ICG Labeling kit-NH2 was purchased from Dojindo Molecular Technologies, Inc. (Rockville, MD, United States). Labeling of antibody with ICG was performed according to the manufacturer's manual. A component of this kit, NH2-reactive ICG, has a succinimidyl ester group and can easily form a covalent bond with an amino group of the antibody. Briefly, NH2-reactive dyes were added to anti-TF antibody (130 μg) solution on the membrane of a filtration tube and incubated at 37 ℃ for 10 min. The buffer solution was then added to the mixture and centrifuged. The conjugate was recovered by pipetting with phosphate-buffered saline (PBS). The concentration of the conjugates was determined

by Bradford protein assay using a BioRad microplate reader (Bio-Rad Laboratrories, Inc., Hercules, CA, United States). The absorbance of ICG was measured at 800 nm with the Synergy HT multi-mode microplate reader (BioTek Instrument, Inc., Winooski, VT, United States), and the number of fluorophore molecules conjugated to each antibody was calculated. The ratio of ICG to antibody was 0.4.

Fluorescence microscopy studies

Fluorescence microscopy was employed to observe the localization of 1849-ICG and the cytotoxic effect of PIT. BxPC-3 or SUIT-2 cells were plated on a Lab-Tek Chamber slide (Thermo Fisher Scientific, Frederick, MD, United States) and incubated for 18 h. Subsequently, culture media were discarded, and the cells were immediately stained after fixation with cold methanol for 5 min at -20 ℃. Nonspecific binding of the antibody was blocked by incubating with Block-Ace reagent (Dainippon Pharmaceutical, Osaka, Japan) solution containing 10% goat serum for 30 min at room temperature. Subsequently, the cells were incubated with the 1849-ICG diluted (1:100) in antibody diluent buffer (Dako, Glostrup, Denmark) or without antibody, at 4 ℃. After 18 h, cells were washed with Tris-buffered saline (TBS), and the nuclei were stained with 4,6-diamidino-2-phenylindole Fluoromount-G (SourthenBiotech, Birmingham, AL, United States). The cells were visualized under a Keyence BZ-X700 microscope (Keyence Japan Co, Ltd, Osaka, Japan) equipped with the following filter sets: excitation wavelength 675 to 750 nm, emission wavelength 760 to 860 nm and dichroic mirror wavelength 760 nm for ICG. To compare BxPC-3 and SUIT-2 cells, images were acquired using the same settings of exposure time and black balance. Phase-contrast images were also acquired.

Cell viability imaging assay after PIT

BxPC-3 cells (2×10^5/well) were seeded in a chamber slide. After 6 h, the culture medium was changed to fresh medium containing 1849-ICG (2.5 μg/mL medium) or not. After an overnight incubation, the culture medium was replaced with phenol red free medium and the cells were subsequently irradiated with NIR light from an Infrared Diode Laser system (Laser Create Co., Tokyo, Japan) at a wavelength of 808 ± 3 nm and a power density of 50 J/cm^2 (1 W/cm^2 for 50 s). The irradiation dose was measured with a thermal laser power sensor and an optical power meter, Starlite (OPHIR Japan, Saitama, Japan). Two hours later, two color staining assay using ReadyProbes™ Cell Viability Imaging kit (Thermo Fisher Scientific) was performed. As per manufacturer's instruction, nuclei of all viable cells were stained with NucBlue® Live reagent, while only the nuclei of dead cells were stained with NucGreen® Dead reagent. The cells were imaged under a Keyence BZ-X700 microscope (Keyence Japan Co, Ltd) equipped with appropriate filter sets for DAPI (excitation/emission maxima: 360/460 nm), GFP (green) filter set (excitation/emission maxima:

470/525 nm) and ICG (excitation/emission maxima: 710/810 nm).

Animal and tumor model

A single-cell suspension of 5×10^6 BxPC-3 cells in 100 μL RPMI medium was mixed with BD Matrigel matrix (BD Biosciences, Bedford, MA, United States) and subcutaneously inoculated into both thighs of 7-wk-old male, BALB/cA Jcl-nu/nu nude mice (CLEA, Shizuoka, Japan) for *in vivo* imaging and NIR-PIT studies. During the experimental procedure, mice were anesthetized with isoflurane. All animal experiments were conducted in compliance with the guidelines for animal experimentation approved by the Animal Care and Use Committee of our institution, National Institute of Radiological Sciences.

In vivo NIR fluorescence imaging

Tumor-bearing mice were injected intravenously with 1849-ICG (100 μg) *via* a tail vein. The mice were anesthetized by inhalation of 2.5% isoflurane, and spectral fluorescence images at dorsal position were obtained using the Maestro *In-vivo* Imaging system (CRi, Woburn, MA, United States) with the ICG filter sets (excitation, 700–770 nm and emission, 790 nm long pass) at pre-injection, followed by various time points post-injection (24, 48, 72, and 144 h). The tunable filter was automatically stepped up in 10-nm increments from 780 to 950 nm for the ICG filter setting, while the camera sequentially captured images at each wavelength interval. With the commercial Maestro software (CRi), subtractions of background and baseline intensities, followed by un-mixing of spectral fluorescence images were performed a step by step. By setting the auto calculate threshold, the region of interest on entire tumors of the ICG spectrum image were determined and the tumor fluorescence signal intensities (FI) were measured. The constant exposure time was set to compare the FI of the serial images. Overlaid image of ICG spectrum image and white light image was acquired by using Photoshop software (Adobe, San Jose, CA, United States).

In vivo PIT of tumor

When the subcutaneous BxPC-3 tumors in mice reached approximately 10 mm at the longest diameter, the tumor-bearing mice were randomly assigned to one of the 5 groups (*n* = 6 for each group) for the treatment study conducted as per the shown scheme (Figure 1). Mice were initially injected 1849-ICG (100 μg) intravenously. On day 1 and day 2, the tumor was irradiated with NIR light from an Infrared Diode Laser system (Laser Create Co.) at a wavelength of 808 ± 3 nm and a power density of 50 J/cm^2 (1 W/cm^2 for 50 s), as measured with a StarLite Laser Power meter (OPHIR Japan Ltd.). During irradiation, the surrounding areas of tumors were shielded from light using aluminum foil. Briefly, group (1) received 1849-ICG i.v. administration followed by two doses of irradiation on two consecutive days, group (2)
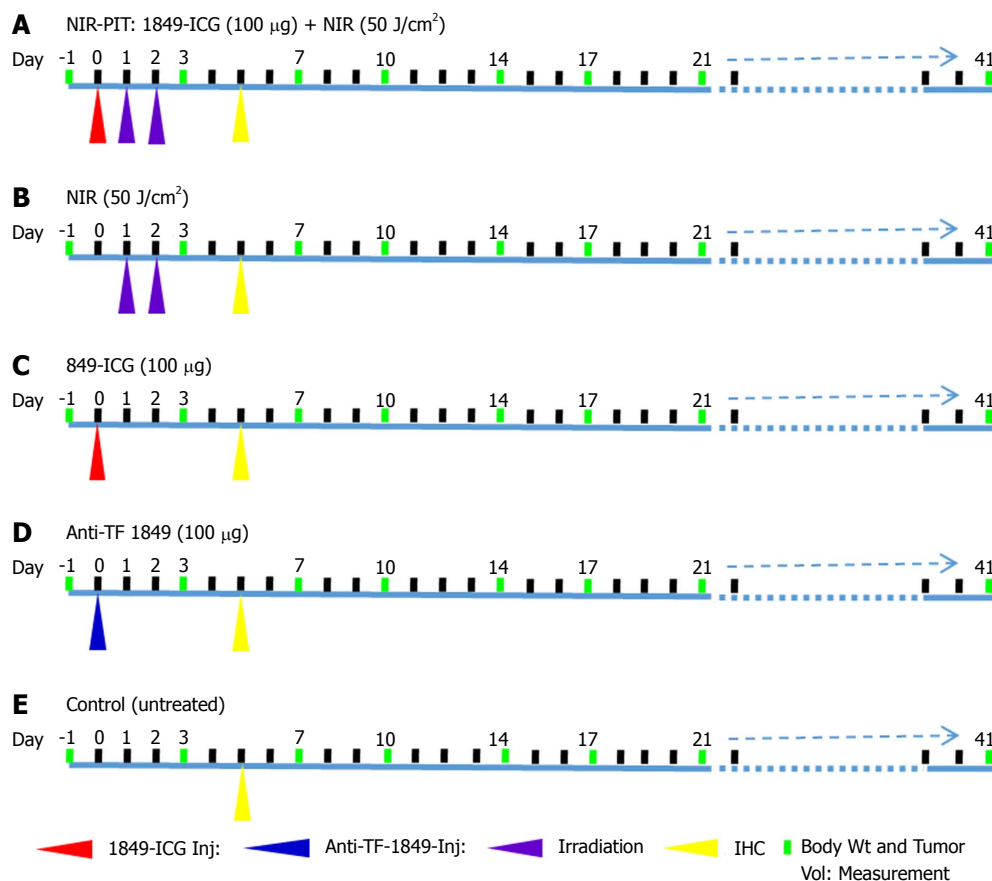
Figure 1 Experimental treatment scheme. A: Near-infrared photoimmunotherapy (NIR-PIT); B: NIR light alone; C: Indocyanine green-labeled antibody 1849 conjugate alone; D: Anti-tissue factor antibody 1849 alone; E: Control (untreated). Anti-TF 1849: Anti-tissue factor antibody 1849; 1849-ICG: Indocyanine green-labeled anti-tissue factor antibody 1849; NIR: Near-infrared; NIR-PIT: Near-infrared photoimmunotherapy.

received two doses of irradiation only on two consecutive days, group (3) received 1849-ICG i.v administration only, group (4) received unlabeled anti-TF 1849 i.v. administration, and group (5) received no treatment. To determine the tumor response, tumors of mice ($n = 12$ for each group except $n = 11$ in anti-TF 1849 group) were measured twice a week throughout the experiment using calipers, and volumes were approximated using the formula: volume (mm^3) = [length (mm)] × [width (mm)]^2 × 0.5. Relative tumor volume was calculated as the volume on the indicated day divided by the starting volume on the day prior to the treatment. Body weight of mice was also measured twice a week; general health conditions and local skin condition at the irradiated area of mice were monitored daily.

Histological and immunohistochemical analysis

At 72 h after 2nd irradiation of NIR-PIT, 2 mice from each group ($n = 2$) were euthanized by cervical dislocation under anesthesia (isoflurane). Tumors were excised from these mice, fixed in 4% paraformaldehyde, and embedded in paraffin. To observe the histologic changes, paraffin-embedded tissues were cut into 5-μm slice, serial sections were fixed on glass slides and stained with hematoxylin and eosin (H&E) staining. To perform immunohistochemical (IHC) analysis, tissue sections

were rehydrated, and subjected to antigen retrieval. The sections were stained for Ki-67, a cell proliferation marker[18], using an anti-human Ki-67 polyclonal antibody (Dako Denmark, Glostrup, Denmark), as previously described[19]. Slides were analyzed using the Olympus BX43 microscope system (Olympus, Tokyo, Japan).

Statistical analysis

All results were expressed as mean ± SD. Significant differences between groups were determined by Student's *t*-test (Excel, Microsoft, Redmond, WA, United States). Two-tailed unpaired *t*-test was used for comparisons of relative tumor volume. The probability of survival based on relative tumor volume (3.1-fold increase of individual tumor volume from the initial volume) was estimated in each group with a Kaplan-Meier survival curve analysis, and the results were compared with use of the Gehan-Breslow-Wilcoxon test. *P*-values < 0.05 were considered significant.

RESULTS

Expression of TF in human pancreatic cancer cell lines

Expression of human TF protein in BxPC-3 and SUIT-2 pancreatic cancer cells was determined through western blot analysis and fluorescence microscopy. In western
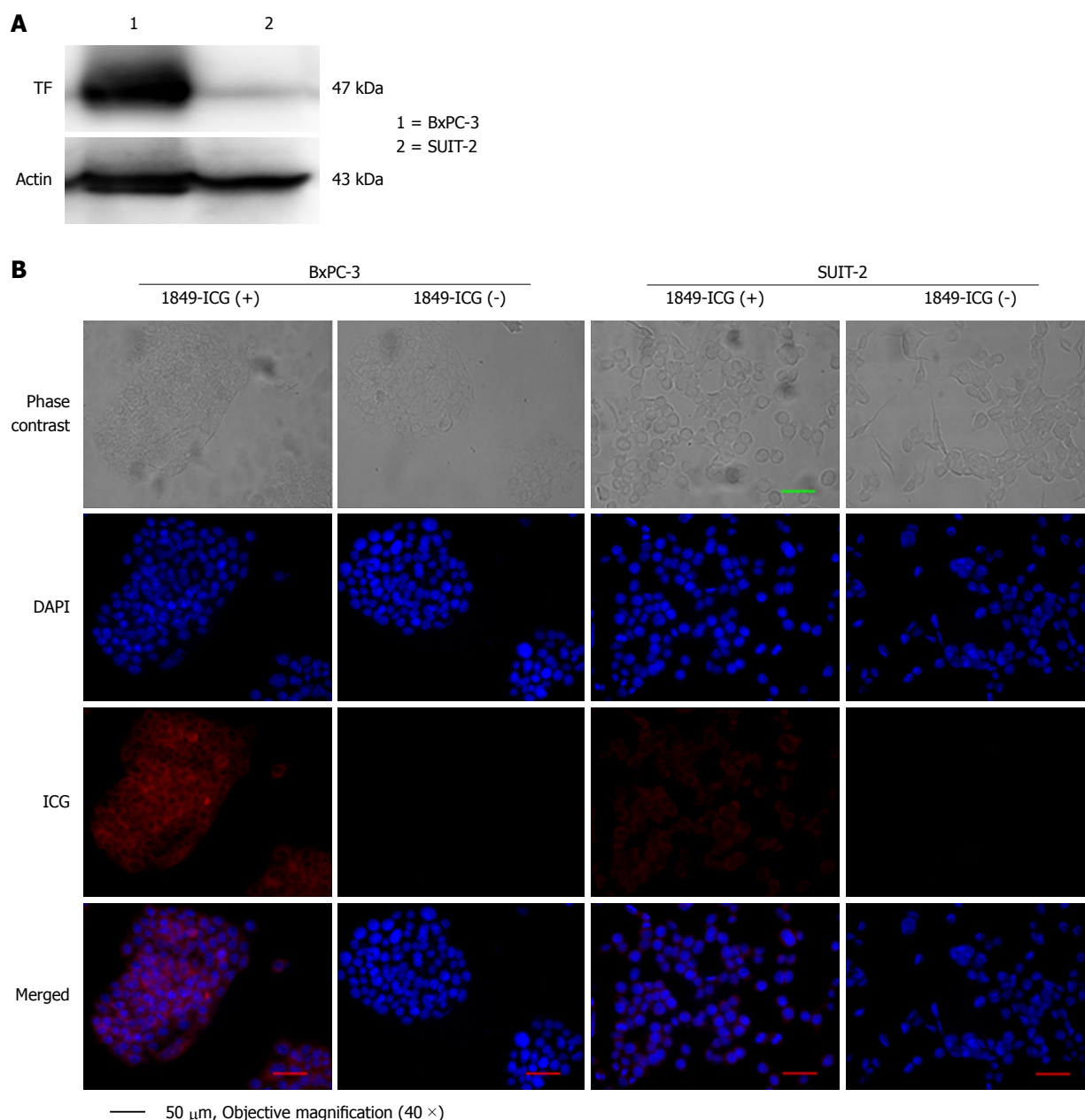
Figure 2 Tissue factor expression in human pancreatic cancer cell lines. A: Tissue factor (TF) expression in the cell lines BxPC-3 (lane 1) and SUIT-2 (lane 2) was examined by western blotting; B: Both cell lines were incubated with or without indocyanine green-labeled anti-TF antibody 1849 (1849-ICG) for 18 h and examined under a fluorescent microscope. Intracellular localization of intense fluorescent signals indicated substantial binding and internalization of 1849-ICG within BxPC-3, but very rarely in SUIT-2 cells (Scale bar = 50 μm, 40 × objective magnification). DAPI: 4,6-diamidino-2-phenylindole; 1849-ICG: Indocyanine green-labeled anti-tissue factor antibody 1849; TF: Tissue factor.

blot analysis of cell lysate, TF expression was found to be much higher in BxPC-3 cells than in SUIT-2 cells (Figure 2A). Moreover, fluorescence microscopy after overnight incubation with 1849-ICG revealed that the preferential binding with intracellular localization of 1849-ICG was higher in BxPC-3 cells than SUIT-2 cells (Figure 2B). Taken together, our data indicated the specific binding of the 1849-ICG conjugate antibody to the highly-expressed TF in BxPC-3 pancreatic cancer cells.

Phototoxic cell death in response to TF-ICG mediated PIT

PIT induced rapid cell death, and numerous dead cells stained with NucGreen® Dead reagent were visualized (Figure 3). Meanwhile, there was no significant cyto-toxicity associated with exposure of 1849-ICG or NIR light exposure alone, in the absence of each other (Figure 3).

In vivo tumor visualization by NIR fluorescence imaging

Mice with subcutaneous BxPC-3 tumors were intra-venously injected with 1849-ICG, followed by NIR fluore-scence imaging at the indicated time points (24, 48, 72, 96 and 144 h after injection). In the untreated group, tumors showed highest FI 24 h after injection and fairly retained the FI until 144 h, our last observation time
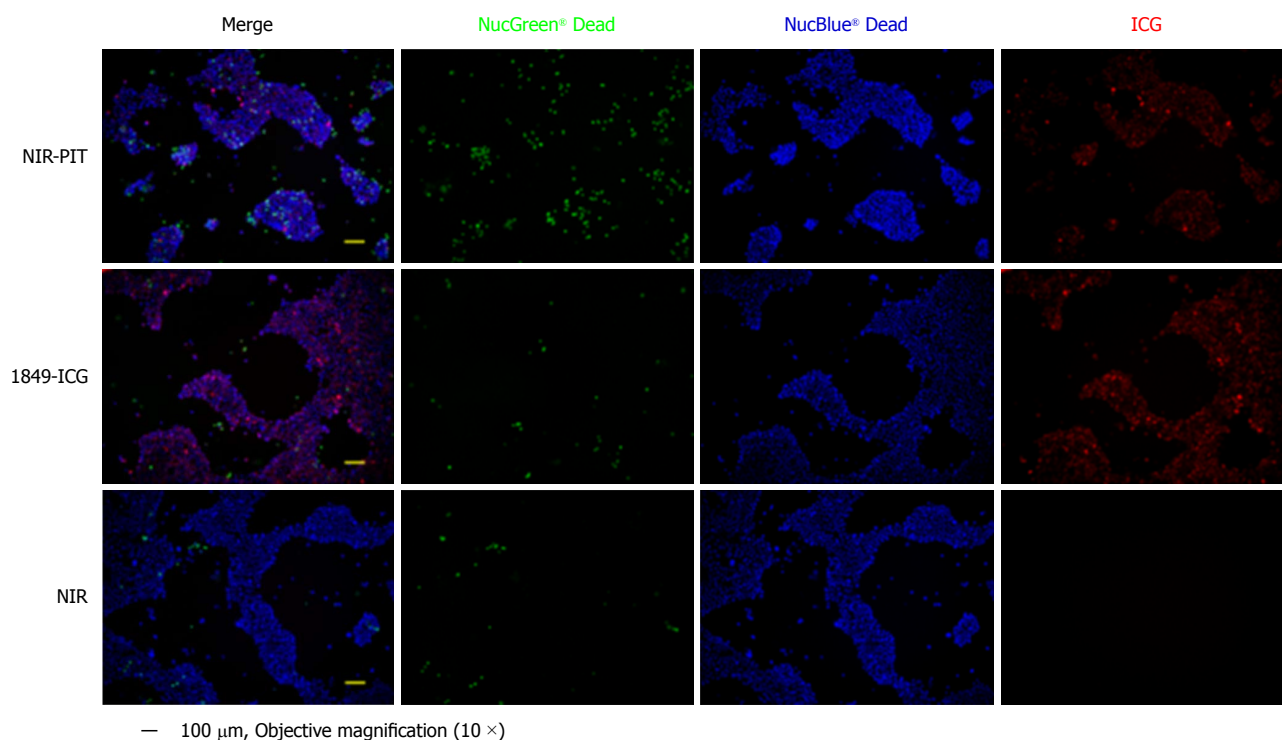
— 100 μm, Objective magnification (10 ×)

Figure 3 Phototoxic cell death after photoimmunotherapy. Two hours after photoimmunotherapy (PIT) treatment, the cells were stained using the Cell viability imaging kit. The nuclei of dead cells were stained with NucGreen® Dead reagent (green), while the viable cell nuclei were stained with NucBlue® Live reagent (blue). Near-infrared (NIR)-PIT induced rapid cell death and numerous dead cells were markedly visible. There was no significant cytotoxicity associated with exposure to indocyanine green-labeled anti-tissue factor antibody 1849 or NIR light only. (Scale bar = 100 μm, 10 × objective magnification). 1849-ICG: Indocyanine green-labeled anti-tissue factor antibody 1849; NIR: Near-infrared; PIT: Photoimmunotherapy.

point, even though FI of tumor decreased gradually over time in longitudinal imaging (Figure 4A). In contrast, the FI of tumors in the PIT group decreased immediately after receiving the irradiation but it increased again in 24 h (Figure 4B).

PIT effects on the tumor growth in nude mice
Tumor growth was significantly inhibited by NIR-PIT with statistically significant differences in the relative tumor volumes for 27 d after the treatment onset when compared to the other groups (no treatment, 1849-ICG only, anti-TF 1849 only and NIR irradiation only) ($P < 0.05$) (Figure 5A). No significant therapeutic effect was observed in the control groups. A significantly prolonged survival was observed in the NIR-PIT group ($P < 0.05$ *vs* the other groups) (Figure 5B). No body weight change (Figure 5C), skin damage, or abnormal general condition were observed in these mice.

Evaluation of the PIT effects with histological and IHC analysis
According to our histological examination and some previous studies, the cells in BxPC-3 tumors have been observed to form a nest pattern, surrounded by stromal tissues in BxPC-3 tumors[20]. However, H&E-stained sections of tumors treated with PIT revealed necrotic death-associated features, such as loss of tumor cells and the nest pattern, scattering of damaged and hypertrophic tumor cells, and marked interstitial fibrosis (Figure 6). On

the other hand, no obvious damage was observed in the tumors of the control groups: receiving only 1849-ICG but no NIR irradiation, receiving only NIR irradiation, receiving only unconjugated anti-TF 1849, and receiving no treatment (Figure 6). As per the IHC examination, the numbers of Ki-67-positive tumor cells, indicating active proliferation, decreased noticeably in the tumor tissues of mice treated with PIT, when compared with the other groups (Figure 7).

DISCUSSION

For cancer therapy, conventional PDT has been suggested as one of the treatment modalities[21]. In PDT, tumor targeting of photosensitizers depends primarily upon the passive enhanced permeability and retention (EPR) effect[22]. However, EPR-based tumor targeting alone faces intrinsic limitations in its specificity and efficacy[23]. To overcome this ambiguity, active targeting strategies using special molecules (antibodies, ligands, *etc.*), which bind to tumor antigens specifically, have been exploited and are preferred as a drug delivery system. Recently, Mitsunaga *et al*[24] and others recommended cancer cell-selective NIR-PIT to overcome the limitation of conventional PDT. Their studies revealed that NIR-PIT induces reliable cytotoxic and antitumor effects in several tumors and derived cell lines[25-32]. Researchers labeled the different types of tumor-specific antibodies such as anti-EGFR mAb[25,26], anti-CD20 mAb[27], anti-

A

B
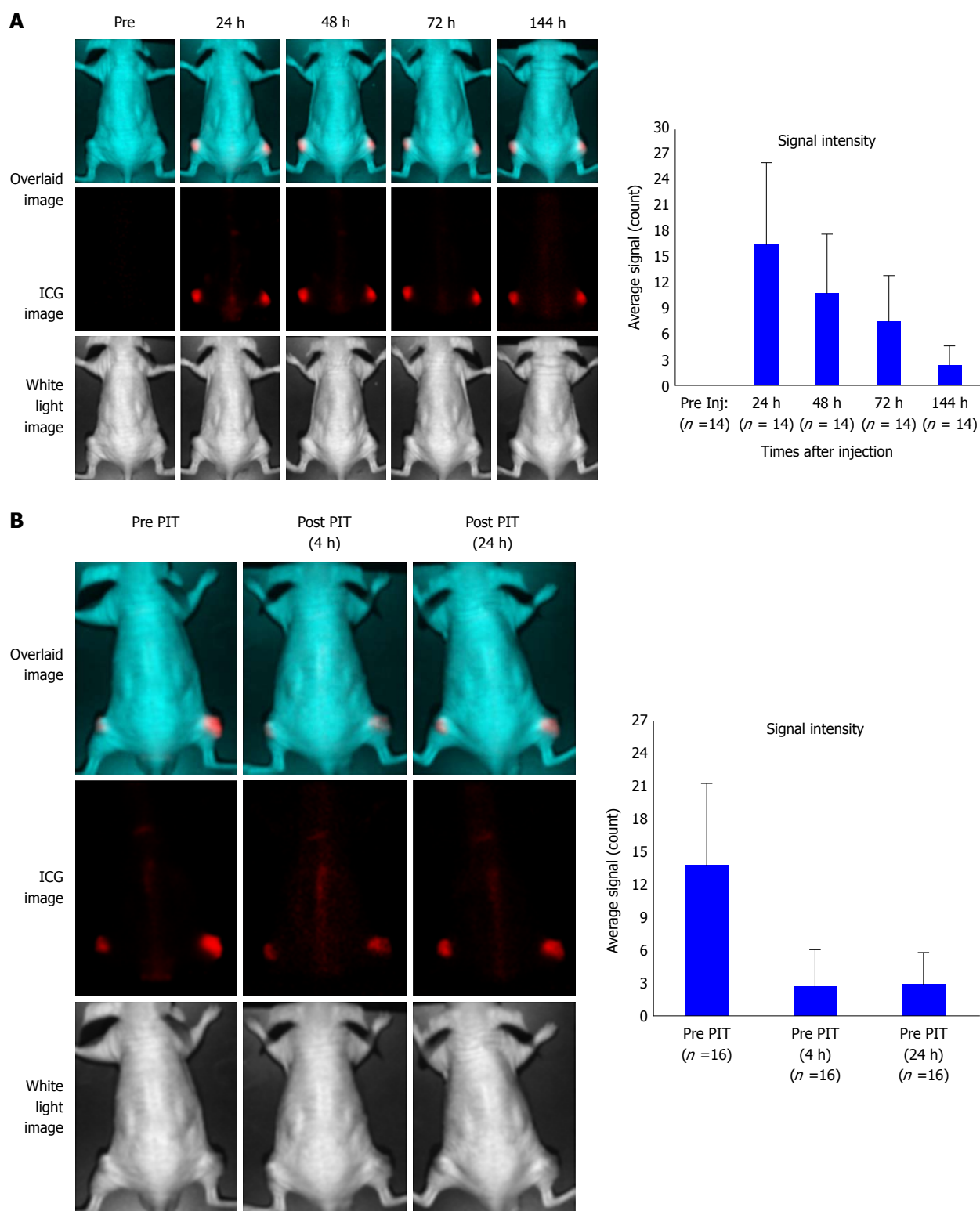
Figure 4 Serial near-infrared fluorescence imaging of a representative mouse bearing xenografted tumor. A: Imaging was performed pre- and post- injection of indocyanine green (ICG)-labeled anti-tissue factor antibody 1849 (1849-ICG) at indicated time points (24, 48, 72, and 144 h). The upper panel shows the overlaid image of the ICG spectrum image (middle panel) and the white light image (lower panel). Fluorescent signal intensity of BxPC-3 tumors is higher than that of the whole body. Adjoining bar graph shows the ICG specific signal intensity of the tumors over time with the peak intensity at 24 h after the injection. Data are presented as mean ± SD (*n* = 14); B: Images of tumor bearing mice before photoimmunotherapy (PIT) (left); 2 h (center) and 24 h (right) after PIT. ICG signal intensity in the tumor decreased initially after PIT and was restored in 24 h suggesting re-accumulation of 1849-ICG due to circulating 1849-ICG. Bar graph shows the ICG signal intensity of tumor before and after near-infrared-PIT. Data are presented as mean ± SD (*n* = 16). 1849-ICG: Indocyanine green-labeled anti-tissue factor antibody 1849; NIR: Near-infrared; PIT: Photoimmunotherapy.

CD44 mAb[33], anti-PD-L1 mAb[34], anti-PSMA mAb[30], anti-CD25 mAb[35], and anti-CEA mAb[31,32], with photo-sensitizer IR700DX, and used them as PIT agents. Although PIT is a promising therapeutic option, very few

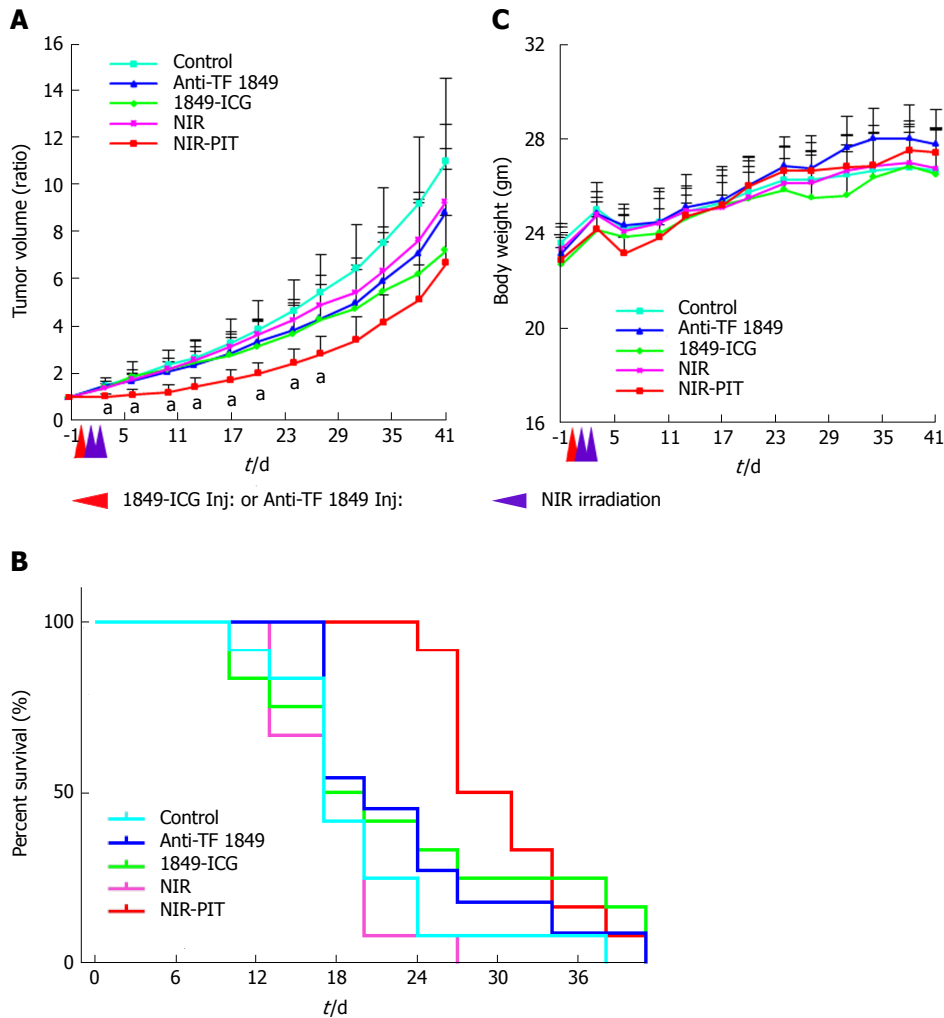**Figure 5 Photoimmunotherapeutic effects on BxPC-3 xenografts and body weight change in mice.** A: Tumor volume change is expressed as the ratio of the volume on the indicated day and volume at 1 d before the start of near-infrared photoimmunotherapy (NIR-PIT). Tumors treated by NIR-PIT (red) showed significantly reduced growth rates compared to those, that received no treatment (light blue), NIR light exposure alone (pink), indocyanine green-labeled anti-tissue factor (TF) antibody 1849 (1849-ICG) alone (green) and anti-TF antibody 1849 (anti-TF 1849) alone (blue), for 27 d after the treatment start date. Values shown represent mean ± SD, $^{a}P < 0.05$, NIR-PIT vs other groups ($n = 12$ for each group except $n = 11$ in anti-TF 1849 group); B: Significantly prolonged survival was observed in NIT-PIT group vs other groups, $^{b}P < 0.05$, by Gehan-Breslow-Wilcoxon test ($n = 12$ for each group except $n = 11$ in anti-TF 1849 group); C: The average body weight did not differ significantly among all 5 groups of mice. Red arrowhead indicates the day of administration of 1849-ICG or Anti-TF 1849 and purple arrowheads indicate the day of NIR exposure. Anti-TF 1849: Anti-tissue factor antibody 1849; 1849-ICG: Indocyanine green-labeled anti-tissue factor antibody 1849; NIR: Near-infrared; PIT: Photoimmunotherapy.

PIT agents have been developed and examined. There-fore, there is a need to develop more PIT agents for treating various cancer patients.

High TF expression is commonly observed in a variety of solid tumors including pancreatic cancer and is associated with poor prognosis of pancreatic ductal adenocarcinoma[36]. Previously, we developed the anti-TF 1849, which has high affinity against TF, and succeeded to visualize TF-expressing tumors noninvasively, in an orthotopic glioma mouse model[13] and pancreatic xeno-graft tumor models (manuscript under preparation) by utilizing the ^{111}In-labeled anti-TF 1849. In the present study, we propose that TF is an attractive molecular target, and evaluate the photoimmunotherapeutic effect mediated by anti-TF 1849 labeled with a photosensitizing fluorophore ICG that is activated and cytotoxic upon irradiation with NIR light.

Our western blot analysis demonstrated the higher expression of TF in BxPC-3 pancreatic cancer cells com-pared to the SUIT-2 cells (Figure 2A). Other researchers have also reported the expression of TF in certain human pancreatic cancer cell lines[10]. These results encouraged us to use BxPC-3 as a representative TF-expressing pancreatic cancer model. Moreover, our results from *in vitro* and *in vivo* fluorescence imaging after overnight incubation of cells with 1849-ICG (Figure 2B) and tumor-bearing mice after 1849-ICG injection, respectively (Figure 4A), showed a strong ICG fluorescence signal in BxPC-3 cells and tumors; indicating the significantly increased accumulation of 1849-ICG in these cells and tumors. Therefore, we hypothesized that our pan-creatic cancer xenograft expressed elevated levels of TF and would be bound specifically with 1849-ICG. Accumulation of 1849-ICG in tumors with fluorescence
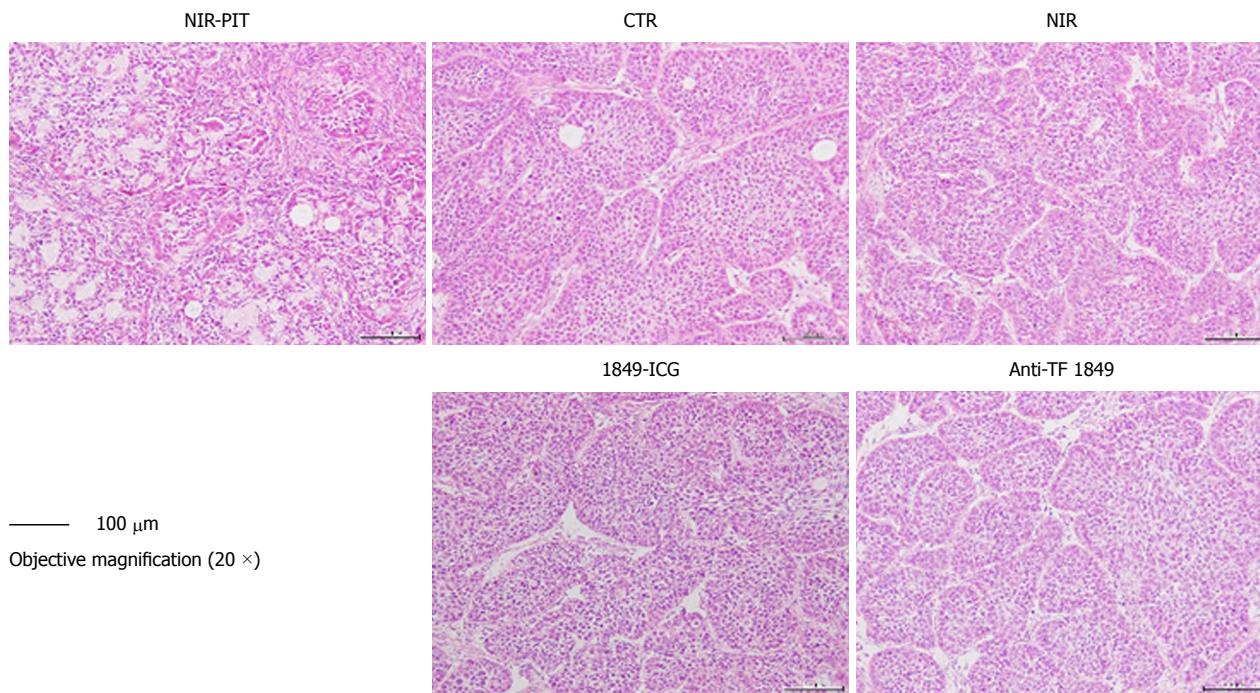
Figure 6 Histological examination of effects of near-infrared photoimmunotherapy 72 h after 2nd exposure to near-infrared light. Tumors were resected and stained with hematoxylin and eosin. After near-infrared photoimmunotherapy (NIR-PIT), tumors showed necrotic death-associated features including loss of tumor cells and cells nest pattern, scattering of damaged and hypertrophic tumor cells, and abundant fibrosis. No obvious damage was detected in the tumors of other control groups; receiving no treatment, NIR light alone, indocyanine green-labeled anti-tissue factor (TF) antibody 1849 (1849-ICG) alone and anti-TF antibody 1849 (anti-TF 1849) alone. Photos of tumor section were taken under 20 × objective magnification (scale bar = 100 μm). Anti-TF 1849: Anti-tissue factor antibody 1849; CTR: Control; 1849-ICG: Indocyanine green-labeled anti-tissue factor antibody 1849; NIR: Near-infrared; PIT: Photoimmunotherapy.

Figure 7 Ki-67 immunostaining of tumor sections 72 h after 2nd exposure to near-infrared light in near-infrared photoimmunotherapy. A marked reduction in Ki-67-positive cell numbers was observed in tumors treated with near-infrared photoimmunotherapy, compared with those of other control groups. Tumor section photos were taken under 20 × objective magnification (scale bar = 100 μm). Anti-TF 1849: Anti-tissue factor antibody 1849; CTR: Control; 1849-ICG: Indocyanine green-labeled anti-tissue factor antibody 1849; NIR: Near-infrared; PIT: Photoimmunotherapy.
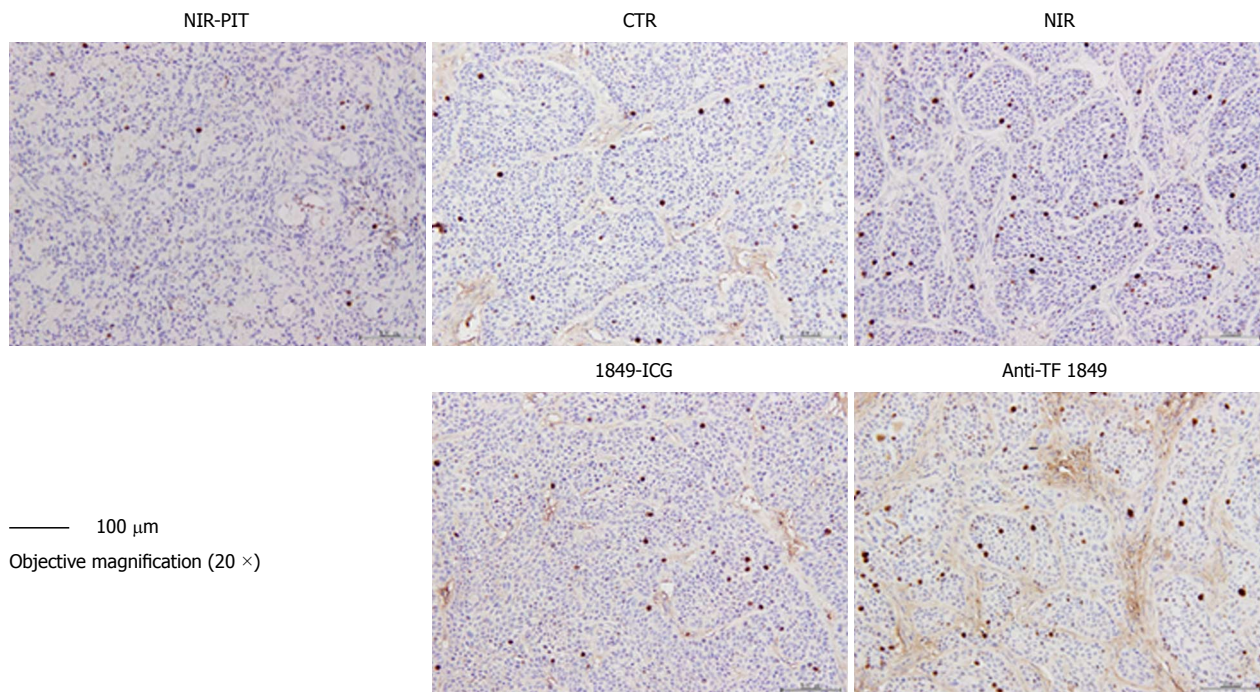
image was serially quantified and was found to peak 24 h after injection. Following NIR-PIT, the ICG signal intensity in the tumor decreased initially, probably due to partial photobleaching of probe and cancer cell death.

Subsequently, the signal intensity tended to increase again, 24 h after PIT, indicating re-accumulation of circulating 1849-ICG in the surviving cells of the residual tumor. This phenomenon may ensure the effect of PIT by additional exposure of NIR 24 h later. Our present study is the first ever report of NIR-PIT targeting TF with 1849-ICG, although there have been studies regarding the targeting of TF for diagnostic imaging[14-16] or radio-isotope therapy[17]. Since TF is expressed not only on tumor cell surface, but also, in tumor stroma[37] and on tumor-associated vascular endothelial cells[38], our NIR-PIT with 1849-ICG may possibly target all of them.

As the NIR-PIT regimen, we used a single 1849-ICG injection followed by NIR light exposure on two consecutive days. We intravenously injected the 100 μg 1849-ICG conjugate in 100 μL PBS to mice and irradiated the tumor with NIR light (50 J/cm^2) on two consecutive days. Even with this treatment regimen, tumor growth retardation was seen, and we could potentially obtain more optimal therapeutic efficacy with minimal adverse effects by increasing the injected dose of conjugate, the irradiation energy, fractionated doses and repeated treatment cycles. There have been reports that NIR-PIT, quickly and massively, kills target-expressing cancer cells within minutes after the NIR light exposure by provoking irreversible cellular membrane damage. As a result, extracellular water can enter the cells, resulting in swelling, blebbing, and rupture of the cells[24]. Moreover, antibody-photosensitizer conjugates selectively bind to target-positive cancer cells with insignificant non-target cellular uptake of the photosensitizer, inducing rapid necrotic damage, especially on cancer cells near blood vessels. Thus, it causes the dilatation of tumor blood vessels and dramatically increasing permeability so called the super EPR (SUPR) effect[39-41]. By means of this phenomenon after the initial NIR-PIT, antibody-photosensitizer conjugates can infiltrate more into the tumor microenvironment with enhanced permeability and penetration after the first dose of NIR-PIT, with a more homogenous access to the surviving cancer cells in tumors[42]. Therefore, an additional irradiation with NIR light can further augment the therapeutic efficacy of NIR-PIT[43].

To comprehensively evaluate the potential effects of 1849-ICG directed NIR-PIT, we performed *in vitro* cell viability imaging assay, longitudinal monitoring of tumor volume change and histological and IHC analyses of tumor sections. NIR-PIT-induced rapid cell death was seen by fluorescence microscopy (Figure 3). Relative tumor volume change showed significant inhibition of tumor growth in the NIT-PIT group compared to the control groups (Figure 4A). In the histological investigation, H&E-stained NIR-PIT-treated tumor sections exhibited necrotic death-associated features (were loss of tumor cells and cells nest pattern, scattering of damaged and hypertrophic tumor cells, and marked interstitial fibrosis), whereas no obvious damage was observed in tumors of the other groups (Figure 6). Furthermore, in the IHC examination, a decrease in number of proliferating cells was noticed in the tumors of mice treated with NIR-PIT (Figure 7). Although rapid and massive cell death was induced by NIR-PIT, to obtain the optimal and prolong antitumor effect, further studies with fractionated dosing of conjugate and repeated exposure of suitable irradiation doses and/or the strategic studies for combining it with other drugs or treatment modalities will be needed.

Kobayashi *et al*[39] and others utilized the IR700DX as the photosensitizer that has photostability, water solubility, and salt tolerance. In the present study, we employed a water-soluble anionic dye ICG as the photosensitizer, which is an already approved fluorescence imaging agent for clinical use by the United States Food and Drug Administration, since a couple of decades because of its safety[44]. Furthermore, the superior features of NIR properties of ICG over other visible fluorophores, such as less auto-fluorescence, better tissue penetration, and large stokes shifts that allow better rejection of excitation light and thus lower background fluorescence[45], encouraged us to use it for *in vivo* NIR imaging and NIT-PIT. NH$_2$-reactive ICG, that we employed here, can easily form a covalent bond with an amino group of anti-TF 1849 without any activation process. Previously, ICG has been reported to be an effective NIR light absorber for laser-mediated photodynamic/PTT[46-48]. Reindl *et al*[49] reported that ICG absorbs 800-nm NIR light, and nearly 90% of the absorbed light is converted to heat. Moreover, there were additional reports about that ICG induces photo-oxidative cell death mediated by a singlet oxygen[50] and heat generation[51]. Thus, photothermal effect and oxidative stress are involved in the mechanisms resulting in the anti-tumor effect of ICG-NIR therapy. The present study demonstrated that ICG is useful for PIT, suggesting that ICG-labeled antibodies are alternative option in addition to IR700DX-labeled.

In the last few years, with the advantage of tumor specificity of PIT over PDT, studies on PIT have increased, and evidences on NIR-PIT-induced immune responses were being reported[52]. The association of PIT and immune response is an interesting topic and needs to be investigated more extensively. Unfortunately, we could not include this issue in our present study.

The specific binding of the 1849-ICG conjugate with inherent fluorescent nature of ICG, which emits the fluorescence signals in the NIR range, enables using this conjugate in clinical practice for both anti-tumor PIT and *in situ* detection of pancreatic cancer. Thus, in the case of resectable pancreatic cancer, tumor margins may be identified by using the intraoperative or endoscopic/laparoscopic setting of ICG fluorescence imaging tools. Furthermore, PIT can be concurrently conducted as an additional therapy to residual tumor tissues. PIT may also be applied to disseminated peritoneal lesions of pancreatic cancer with minimal damage to surrounding healthy normal tissues. Although, the development of clinically usable devices for endoscopic/laparoscopic fluorescence imaging and NIR-PIT remain a hurdle, there

is a possibility to overcome it with advancing software and hardware technologies.

In conclusion, the current study reveals that 1849-ICG conjugate accumulated in a TF-overexpressing pancreatic cancer cell and xenografts model BxPC-3. A single dose of 1849-ICG conjugate administration accompanied by NIR light exposure (50 J/cm^2) for two consecutive days effectively inhibited tumor growth *in vivo* without producing any noticeable adverse effects. Taken together, our results suggest that NIR-PIT employing TF as a targeting antigen for the 1849-ICG is a promising new treatment modality for pancreatic cancer with a useful contemporaneous diagnostic utility, which could be ultimately applicable in clinical use.

ARTICLE HIGHLIGHTS

Research background
Pancreatic cancer is still one of major life-threatening diseases. Therefore, there is an urgent need to explore early diagnostic and new therapeutic options. Near infrared photoimmunotherapy (NIR-PIT) is a highly selective tumor treatment that utilizes antibody-photosensitizer conjugate systemic administration, accompanied by subsequent NIR light exposure. Tissue factor (TF) is a transmembrane protein and its overexpression is associated with increased tumor growth, tumor angiogenesis and metastatic potential in many malignancies, including pancreatic cancer.

Research motivation
Previously, we suggested that TF may be a promising target for cancer diagnostic imaging probe and have already reported the usefulness of anti-TF monoclonal antibody (anti-TF mAb) in cancer imaging and therapy. However, NIR-PIT using anti-TF mAb has not been attempted.

Research objectives
In this study, we aim to investigate the photoimmunotherapeutic effect induced by a rat IgG$_{2b}$ anti-TF monoclonal antibody 1849 (anti-TF 1849), conjugated to the NIR photosensitizer, indocyanine green (ICG), in a TF-expressing BxPC-3 pancreatic cancer model.

Research methods
An ICG-labeled antibody conjugate (1849-ICG) was generated by labeling an anti-TF 1849 with ICG. The expression levels of TF in two human pancreatic cancer cell lines were examined by western blotting. Specific binding of the 1849-ICG to BxPC-3 cells was examined by fluorescence microscopy. NIR-PIT-induced cell death was determined by cell viability imaging assay. *In vivo* longitudinal fluorescence imaging was used to explore the accumulation of 1849-ICG conjugate in xenograft tumors. To determine the effect of NIR-PIT, tumor-bearing mice were divided into 5 groups: (1) 100 μg of 1849-ICG i.v. administration followed by NIR light exposure (50 J/cm^2) on two consecutive days (Days 1 and 2); (2) NIR light exposure (50 J/cm^2) only on two consecutive days (Days 1 and 2); (3) 100 μg of 1849-ICG i.v. administration; (4) 100 μg of unlabeled anti-TF 1849 i.v. administration; and (5) the untreated control. Semiweekly tumor volume measurements, accompanied with histological and immunohistochemical (IHC) analyses of tumors, were performed 3 d after the 2nd irradiation with NIR light to monitor the effect of treatments.

Research results
High TF expression in BxPC-3 cells was observed *via* western blot analysis, concordant with the observed preferential binding with intracellular localization of 1849-ICG *via* fluorescence microscopy. NIR-PIT-induced cell death was observed by performing cell viability imaging assay. In contrast to the other test groups, tumor growth was significantly inhibited by NIR-PIT with a statistically significant difference in relative tumor volumes ($P < 0.05$). Tumors that received NIR-PIT showed evidence of necrotic cell death-associated features upon hematoxylin-eosin staining accompanied by a decrease in Ki-67-positive cells (a

cell proliferation marker) by IHC examination.

Research conclusions
The TF-targeted NIR-PIT with the 1849-ICG conjugate can potentially open a new platform for treatment of TF-expressing pancreatic cancer.

Research perspectives
Because TF-targeted NIR-PIT is a promising new treatment modality with a useful contemporaneous diagnostic utility, we will approach to apply it in clinical use. In addition, the association of PIT and immune response is an interesting topic and we will explore it in the future study.

REFERENCES

1 **GBD 2015 Mortality and Causes of Death Collaborators**. Global, regional, and national life expectancy, all-cause mortality, and cause-specific mortality for 249 causes of death, 1980-2015: a systematic analysis for the Global Burden of Disease Study 2015. *Lancet* 2016; **388**: 1459-1544 [PMID: 27733281 DOI: 10.1016/S0140-6736(16)31012-1]

2 **Siegel RL**, Miller KD, Jemal A. Cancer statistics, 2018. *CA Cancer J Clin* 2018; **68**: 7-30 [PMID: 29313949 DOI: 10.3322/caac.21442]

3 **Kasthuri RS**, Taubman MB, Mackman N. Role of tissue factor in cancer. *J Clin Oncol* 2009; **27**: 4834-4838 [PMID: 19738116 DOI: 10.1200/JCO.2009.22.6324]

4 **van den Berg YW**, Osanto S, Reitsma PH, Versteeg HH. The relationship between tissue factor and cancer progression: insights from bench and bedside. *Blood* 2012; **119**: 924-932 [PMID: 22065595 DOI: 10.1182/blood-2011-06-317685]

5 **Leppert U**, Eisenreich A. The role of tissue factor isoforms in cancer biology. *Int J Cancer* 2015; **137**: 497-503 [PMID: 24806794 DOI: 10.1002/ijc.28959]

6 **Kakkar AK**, Lemoine NR, Scully MF, Tebbutt S, Williamson RC. Tissue factor expression correlates with histological grade in human pancreatic cancer. *Br J Surg* 1995; **82**: 1101-1104 [PMID: 7648165 DOI: 10.1002/bjs.1800820831]

7 **Ueda C**, Hirohata Y, Kihara Y, Nakamura H, Abe S, Akahane K, Okamoto K, Itoh H, Otsuki M. Pancreatic cancer complicated by disseminated intravascular coagulation associated with production of tissue factor. *J Gastroenterol* 2001; **36**: 848-850 [PMID: 11777214]

8 **Khorana AA**, Ahrendt SA, Ryan CK, Francis CW, Hruban RH, Hu YC, Hostetter G, Harvey J, Taubman MB. Tissue factor expression, angiogenesis, and thrombosis in pancreatic cancer. *Clin Cancer Res* 2007; **13**: 2870-2875 [PMID: 17504985 DOI: 10.1158/1078-0432.CCR-06-2351]

9 **Hobbs JE**, Zakarija A, Cundiff DL, Doll JA, Hymen E, Cornwell M, Crawford SE, Liu N, Signaevsky M, Soff GA. Alternatively spliced human tissue factor promotes tumor growth and angiogenesis in a pancreatic cancer tumor model. *Thromb Res* 2007; **120** Suppl 2: S13-S21 [PMID: 18023707 DOI: 10.1016/S0049-3848(07)70126-3]

10 **Haas SL**, Jesnowski R, Steiner M, Hummel F, Ringel J, Burstein C, Nizze H, Liebe S, Löhr JM. Expression of tissue factor in pancreatic adenocarcinoma is associated with activation of coagulation. *World J Gastroenterol* 2006; **12**: 4843-4849 [PMID: 16937466]

11 **Tsumura R**, Sato R, Furuya F, Koga Y, Yamamoto Y, Fujiwara Y, Yasunaga M, Matsumura Y. Feasibility study of the Fab fragment of a monoclonal antibody against tissue factor as a diagnostic tool. *Int J Oncol* 2015; **47**: 2107-2114 [PMID: 26497165 DOI: 10.3892/ijo.2015.3210]

12 **Koga Y**, Manabe S, Aihara Y, Sato R, Tsumura R, Iwafuji H, Furuya F, Fuchigami H, Fujiwara Y, Hisada Y, Yamamoto Y, Yasunaga M, Matsumura Y. Antitumor effect of antitissue factor antibody-MMAE conjugate in human pancreatic tumor xenografts. *Int J Cancer* 2015; **137**: 1457-1466 [PMID: 25704403 DOI: 10.1002/ijc.29492]

13 **Takashima H**, Tsuji AB, Saga T, Yasunaga M, Koga Y, Kuroda JI, Yano S, Kuratsu JI, Matsumura Y. Molecular imaging using an anti-human tissue factor monoclonal antibody in an orthotopic glioma xenograft model. *Sci Rep* 2017; **7**: 12341 [PMID: 28951589 DOI: 10.1038/s41598-017-12563-5]

14 **Hernandez R**, England CG, Yang Y, Valdovinos HF, Liu B, Wong

HC, Barnhart TE, Cai W. ImmunoPET imaging of tissue factor expression in pancreatic cancer with [89]Zr-Df-ALT-836. *J Control Release* 2017; **264**: 160-168 [PMID: 28843831 DOI: 10.1016/j.jconrel.2017.08.029]

15   **Hong H**, Zhang Y, Nayak TR, Engle JW, Wong HC, Liu B, Barnhart TE, Cai W. Immuno-PET of tissue factor in pancreatic cancer. *J Nucl Med* 2012; **53**: 1748-1754 [PMID: 22988057 DOI: 10.2967/jnumed.112.105460]

16   **Shi S**, Hong H, Orbay H, Graves SA, Yang Y, Ohman JD, Liu B, Nickles RJ, Wong HC, Cai W. ImmunoPET of tissue factor expression in triple-negative breast cancer with a radiolabeled antibody Fab fragment. *Eur J Nucl Med Mol Imaging* 2015; **42**: 1295-1303 [PMID: 25801992 DOI: 10.1007/s00259-015-3038-1]

17   **Wang B**, Berger M, Masters G, Albone E, Yang Q, Sheedy J, Kirksey Y, Grimm L, Wang B, Singleton J, Soltis D. Radiotherapy of human xenograft NSCLC tumors in nude mice with a 90Y-labeled anti-tissue factor antibody. *Cancer Biother Radiopharm* 2005; **20**: 300-309 [PMID: 15989475 DOI: 10.1089/cbr.2005.20.300]

18   **Scholzen T**, Gerdes J. The Ki-67 protein: from the known and the unknown. *J Cell Physiol* 2000; **182**: 311-322 [PMID: 10653597 DOI: 1 0.1002/(SICI)1097-4652(200003)182:3<311::AID-JCP1>3.0.CO;2-9]

19   **Sudo H**, Tsuji AB, Sugyo A, Ogawa Y, Sagara M, Saga T. ZDHHC8 knockdown enhances radiosensitivity and suppresses tumor growth in a mesothelioma mouse model. *Cancer Sci* 2012; **103**: 203-209 [PMID: 22017350 DOI: 10.1111/j.1349-7006.2011.02126.x]

20   **Kano MR**, Bae Y, Iwata C, Morishita Y, Yashiro M, Oka M, Fujii T, Komuro A, Kiyono K, Kaminishi M, Hirakawa K, Ouchi Y, Nishiyama N, Kataoka K, Miyazono K. Improvement of cancer-targeting therapy, using nanocarriers for intractable solid tumors by inhibition of TGF-beta signaling. *Proc Natl Acad Sci USA* 2007; **104**: 3460-3465 [PMID: 17307870 DOI: 10.1073/pnas.0611660104]

21   **Agostinis P**, Berg K, Cengel KA, Foster TH, Girotti AW, Gollnick SO, Hahn SM, Hamblin MR, Juzeniene A, Kessel D, Korbelik M, Moan J, Mroz P, Nowis D, Piette J, Wilson BC, Golab J. Photodynamic therapy of cancer: an update. *CA Cancer J Clin* 2011; **61**: 250-281 [PMID: 21617154 DOI: 10.3322/caac.20114]

22   **Shirasu N**, Nam SO, Kuroki M. Tumor-targeted photodynamic therapy. *Anticancer Res* 2013; **33**: 2823-2831 [PMID: 23780966]

23   **Peer D**, Karp JM, Hong S, Farokhzad OC, Margalit R, Langer R. Nanocarriers as an emerging platform for cancer therapy. *Nat Nanotechnol* 2007; **2**: 751-760 [PMID: 18654426 DOI: 10.1038/nnano.2007.387]

24   **Mitsunaga M**, Ogawa M, Kosaka N, Rosenblum LT, Choyke PL, Kobayashi H. Cancer cell-selective in vivo near infrared photoimmunotherapy targeting specific membrane molecules. *Nat Med* 2011; **17**: 1685-1691 [PMID: 22057348 DOI: 10.1038/nm.2554]

25   **Burley TA**, Mączyńska J, Shah A, Szopa W, Harrington KJ, Boult JKR, Mrozek-Wilczkiewicz A, Vinci M, Bamber JC, Kaspera W, Kramer-Marek G. Near-infrared photoimmunotherapy targeting EGFR-Shedding new light on glioblastoma treatment. *Int J Cancer* 2018; **142**: 2363-2374 [PMID: 29313975 DOI: 10.1002/ijc.31246]

26   **Nakamura Y**, Ohler ZW, Householder D, Nagaya T, Sato K, Okuyama S, Ogata F, Daar D, Hoa T, Choyke PL, Kobayashi H. Near Infrared Photoimmunotherapy in a Transgenic Mouse Model of Spontaneous Epidermal Growth Factor Receptor (EGFR)-expressing Lung Cancer. *Mol Cancer Ther* 2017; **16**: 408-414 [PMID: 28151706 DOI: 10.1158/1535-7163.MCT-16-0663]

27   **Heryanto YD**, Hanaoka H, Nakajima T, Yamaguchi A, Tsushima Y. Applying near-infrared photoimmunotherapy to B-cell lymphoma: comparative evaluation with radioimmunotherapy in tumor xenografts. *Ann Nucl Med* 2017; **31**: 669-677 [PMID: 28741052 DOI: 10.1007/s12149-017-1197-9]

28   **Railkar R**, Krane LS, Li QQ, Sanford T, Siddiqui MR, Haines D, Vourganti S, Brancato SJ, Choyke PL, Kobayashi H, Agarwal PK. Epidermal Growth Factor Receptor (EGFR)-targeted Photoimmunotherapy (PIT) for the Treatment of EGFR-expressing Bladder Cancer. *Mol Cancer Ther* 2017; **16**: 2201-2214 [PMID: 28619755 DOI: 10.1158/1535-7163.MCT-16-0924]

29   **Jin J**, Krishnamachary B, Mironchik Y, Kobayashi H, Bhujwalla ZM. Phototheranostics of CD44-positive cell populations in triple negative breast cancer. *Sci Rep* 2016; **6**: 27871 [PMID: 27302409 DOI: 10.1038/srep27871]

30   **Nagaya T**, Nakamura Y, Okuyama S, Ogata F, Maruoka Y, Choyke PL, Kobayashi H. Near-Infrared Photoimmunotherapy Targeting Prostate Cancer with Prostate-Specific Membrane Antigen (PSMA) Antibody. *Mol Cancer Res* 2017; **15**: 1153-1162 [PMID: 28588059 DOI: 10.1158/1541-7786.MCR-17-0164]

31   **Shirasu N**, Yamada H, Shibaguchi H, Kuroki M, Kuroki M. Potent and specific antitumor effect of CEA-targeted photoimmunotherapy. *Int J Cancer* 2014; **135**: 2697-2710 [PMID: 24740257 DOI: 10.1002/ijc.28907]

32   **Maawy AA**, Hiroshima Y, Zhang Y, Heim R, Makings L, Garcia-Guzman M, Luiken GA, Kobayashi H, Hoffman RM, Bouvet M. Near infra-red photoimmunotherapy with anti-CEA-IR700 results in extensive tumor lysis and a significant decrease in tumor burden in orthotopic mouse models of pancreatic cancer. *PLoS One* 2015; **10**: e0121989 [PMID: 25799218 DOI: 10.1371/journal.pone.0121989]

33   **Nagaya T**, Nakamura Y, Okuyama S, Ogata F, Maruoka Y, Choyke PL, Allen C, Kobayashi H. Syngeneic Mouse Models of Oral Cancer Are Effectively Targeted by Anti-CD44-Based NIR-PIT. *Mol Cancer Res* 2017; **15**: 1667-1677 [PMID: 28923838 DOI: 10.1158/1541-7786.MCR-17-0333]

34   **Nagaya T**, Nakamura Y, Sato K, Harada T, Choyke PL, Hodge JW, Schlom J, Kobayashi H. Near infrared photoimmunotherapy with avelumab, an anti-programmed death-ligand 1 (PD-L1) antibody. *Oncotarget* 2017; **8**: 8807-8817 [PMID: 27716622 DOI: 10.18632/oncotarget.12410]

35   **Nakajima T**, Sano K, Choyke PL, Kobayashi H. Improving the efficacy of Photoimmunotherapy (PIT) using a cocktail of antibody conjugates in a multiple antigen tumor model. *Theranostics* 2013; **3**: 357-365 [PMID: 23781283 DOI: 10.7150/thno.5908]

36   **Nitori N**, Ino Y, Nakanishi Y, Yamada T, Honda K, Yanagihara K, Kosuge T, Kanai Y, Kitajima M, Hirohashi S. Prognostic significance of tissue factor in pancreatic ductal adenocarcinoma. *Clin Cancer Res* 2005; **11**: 2531-2539 [PMID: 15814630 DOI: 10.1158/1078-0432.CCR-04-0866]

37   **Vrana JA**, Stang MT, Grande JP, Getz MJ. Expression of tissue factor in tumor stroma correlates with progression to invasive human breast cancer: paracrine regulation by carcinoma cell-derived members of the transforming growth factor beta family. *Cancer Res* 1996; **56**: 5063-5070 [PMID: 8895765]

38   **Contrino J**, Hair G, Kreutzer DL, Rickles FR. In situ detection of tissue factor in vascular endothelial cells: correlation with the malignant phenotype of human breast disease. *Nat Med* 1996; **2**: 209-215 [PMID: 8574967]

39   **Kobayashi H**, Choyke PL. Super enhanced permeability and retention (SUPR) effects in tumors following near infrared photoimmunotherapy. *Nanoscale* 2016; **8**: 12504-12509 [PMID: 26443992 DOI: 10.1039/c5nr05552k]

40   **Sano K**, Nakajima T, Choyke PL, Kobayashi H. The effect of photoimmunotherapy followed by liposomal daunorubicin in a mixed tumor model: a demonstration of the super-enhanced permeability and retention effect after photoimmunotherapy. *Mol Cancer Ther* 2014; **13**: 426-432 [PMID: 24356818 DOI: 10.1158/1535-7163.MCT-13-0633]

41   **Sano K**, Nakajima T, Choyke PL, Kobayashi H. Markedly enhanced permeability and retention effects induced by photo-immunotherapy of tumors. *ACS Nano* 2013; **7**: 717-724 [PMID: 23214407 DOI: 10.1021/nn305011p]

42   **Nagaya T**, Nakamura Y, Sato K, Harada T, Choyke PL, Kobayashi H. Improved micro-distribution of antibody-photon absorber conjugates after initial near infrared photoimmunotherapy (NIR-PIT). *J Control Release* 2016; **232**: 1-8 [PMID: 27059723 DOI: 10.1016/j.jconrel.2016.04.003]

43   **Mitsunaga M**, Nakajima T, Sano K, Choyke PL, Kobayashi H. Near-infrared theranostic photoimmunotherapy (PIT): repeated exposure of light enhances the effect of immunoconjugate. *Bioconjug Chem* 2012; **23**: 604-609 [PMID: 22369484 DOI: 10.1021/bc200648m]

44   **Dzurinko VL**, Gurwood AS, Price JR. Intravenous and indocyanine green angiography. *Optometry* 2004; **75**: 743-755 [PMID: 15624671]

45   **Sharma R**, Wendt JA, Rasmussen JC, Adams KE, Marshall MV,

Sevick-Muraca EM. New horizons for imaging lymphatic function. *Ann N Y Acad Sci* 2008; **1131**: 13-36 [PMID: 18519956 DOI: 10.1196/annals.1413.002]

46   **Shirata C**, Kaneko J, Inagaki Y, Kokudo T, Sato M, Kiritani S, Akamatsu N, Arita J, Sakamoto Y, Hasegawa K, Kokudo N. Near-infrared photothermal/photodynamic therapy with indocyanine green induces apoptosis of hepatocellular carcinoma cells through oxidative stress. *Sci Rep* 2017; **7**: 13958 [PMID: 29066756 DOI: 10.1038/s41598-017-14401-0]

47   **Tseng WW**, Saxton RE, Deganutti A, Liu CD. Infrared laser activation of indocyanine green inhibits growth in human pancreatic cancer. *Pancreas* 2003; **27**: e42-e45 [PMID: 14508139]

48   **Radzi R**, Osaki T, Tsuka T, Imagawa T, Minami S, Nakayama Y, Okamoto Y. Photodynamic hyperthermal therapy with indocyanine green (ICG) induces apoptosis and cell cycle arrest in B16F10 murine melanoma cells. *J Vet Med Sci* 2012; **74**: 545-551 [PMID: 22146339]

49   **Reindl S,** Penzkofer A, Gong SH, Landthaler M, Szeimies RM, Abels C, Baumler W. Quantum yield of triplet formation for indocyanine green. *J Photoch Photobio A* 1997; **105**: 65-68 [DOI: 10.1016/S1010-6030(96)04584-4]

50   **Bäumler W**, Abels C, Karrer S, Weiss T, Messmann H, Landthaler M, Szeimies RM. Photo-oxidative killing of human colonic cancer cells using indocyanine green and infrared light. *Br J Cancer* 1999; **80**: 360-363 [PMID: 10408838 DOI: 10.1038/sj.bjc.6690363]

51   **Urbanska K**, Romanowska-Dixon B, Matuszak Z, Oszajca J, Nowak-Sliwinska P, Stochel G. Indocyanine green as a prospective sensitizer for photodynamic therapy of melanomas. *Acta Biochim Pol* 2002; **49**: 387-391 [PMID: 12362980]

52   **Ogawa M**, Tomita Y, Nakamura Y, Lee MJ, Lee S, Tomita S, Nagaya T, Sato K, Yamauchi T, Iwai H, Kumar A, Haystead T, Shroff H, Choyke PL, Trepel JB, Kobayashi H. Immunogenic cancer cell death selectively induced by near infrared photoimmunotherapy initiates host tumor immunity. *Oncotarget* 2017; **8**: 10425-10436 [PMID: 28060726 DOI: 10.18632/oncotarget.14425]

Baishideng®